Influence of Sugarcane Bagasse Fiber Size on Biodegradable Composites of Thermoplastic Starch

Bruno Henrique dos Santos, Karen de Souza do Prado, Asaph Armando Jacinto and Márcia Aparecida da Silva Spinacé*

Federal University of ABC, Center of Natural and Human Sciences, Av. dos Estados, 5001, Santa Terezinha, 09.210-170 Santo André, São Paulo, Brazil

ABSTRACT: Although thermoplastic starch (TPS) is biodegradable, its low mechanical resistance limits its wide application. Sugarcane bagasse (SB) fibers can be used as reinforcement in TPS matrix composites, but the influence of fiber size on the properties of the composite is still unknown. In this study, TPS composites reinforced with SB short fibers of four sizes were processed and characterized in order to analyze the influence of fiber size on the mechanical properties of the TPS/SB composite. It was observed that the interaction between fiber and matrix was good and optimized when the fibers are sifted in sieves between 30 and 50 mesh, obtaining fibers with average length of 1569 ± 640 μm and average diameter of 646 ± 166 μm. For these composites, increases of more than 660% in the modulus and more than 100% in the maximum tension were verified when compared to the pure TPS.

KEYWORDS: Sugarcane bagasse, thermoplastic starch, composite, fiber size

1 INTRODUCTION

Sugarcane is one of the most important crops globally and is raw material in several processes, mainly in biofuels production to obtain ethanol and in the food industry to obtain sugar. Brazil is its major producer in the world, reaching more than 650 million tons between 2016 and 2017 [1]. As each ton of sugarcane generates about 280 kg of bagasse [2, 3], there is an increasing concern regarding sugarcane bagasse (SB) disposal in the environment, which may lead to water pollution, formation of dust, unpleasant odor, microbial deposition and even spontaneous ignition [4–6].

To avoid these issues, SB has been reused in many applications, e.g., to produce paper, in the manufacturing of concrete as an additive or for partially replacing cement, or to feed thermoelectric power plants [3, 7, 8]. SB fibers are composed of bundles of elementary fibers, and are mainly made up of cellulose, hemicelluloses and lignin. As cellulose is the major component [9], SB fibers show high tensile strength, which allows their application as reinforcement in polymeric composites [8–11].

Among the possible polymeric matrixes, thermoplastic starch (TPS) has emerged as an interesting alternative because it is not petroleum based and provides high availability, biodegradability and lower cost when compared to the conventional synthetic biodegradable polymers [12]. TPS can be used in packaging applications, but its wide application is still limited due to its water absorption characteristics and poor mechanical properties [13].

The addition of SB fibers from agroindustrial wastes to TPS matrix arises as a cost-effective and environmentally friendly solution to the poor mechanical properties of TPS. The literature reports some studies about TPS/SB composites [8, 14–21], but most of them employ some chemical pretreatment of SB fibers and none are focused on the influence of SB fibers size distribution on the mechanical properties of the composite.

It is well known that fiber size has an important role in the mechanical properties of polymeric composites. In general, for short-fiber-reinforced composites, there is an optimum fiber size to obtain improved properties such as tensile strength [22]. However, it is still not clear whether an optimum fiber size exists that gives the best mechanical properties balance to TPS composites with discontinuous SB fibers.

In this context, the aims of this study are to prepare composites of TPS with different size ranges of SB fibers without chemical pretreatment, and to evaluate the influence of fiber size on the mechanical properties of TPS/SB composites.

2 EXPERIMENTAL

2.1 Materials

Local markets in Santo André (São Paulo, Brazil) supplied the SB waste. Commercial food-grade corn starch (Yoki®), bidistilled glycerin (Synth PA) as plasticizer and deionized water were used for the production of TPS.

2.2 SB Preparation

The SB fibers (Figure 1a) were immersed in deionized water at 23 °C for 36 h, and then washed in running water to remove impurities and soluble sugars. Dried SB fibers (23 °C for 48 h) were ground in a knife mill (Marconi, M048) and sifted in sieves (Contenco) of 28, 48 and 60 mesh (Figure 1b) in order to separate SB fibers of different size ranges (Table 1).

2.3 Composite Preparation

The TPS (Figure 1c) was compounded by 75 wt% of corn starch, 15 wt% of bidistilled glycerin and 10 wt% of deionized water. The mixture was processed in a single screw mini extruder (AX Plásticos) with three
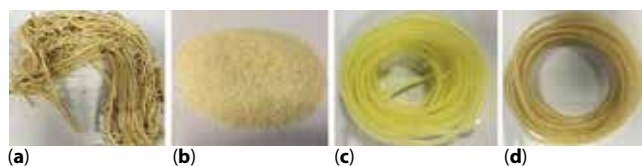

(a)   **(b)**   **(c)**   **(d)**

Figure 1 (**a**) SB fibers, (**b**) milled SB fibers, (**c**) pure TPS and (**d**) TPS/SB composite.

Table 1 Average dimension and aspect ratio (L/D) for each size range of SB fibers.

Sample	Size range (μm)	L (μm)	D (μm)	L/D
SBl	> 595	1944 ± 650	898 ± 26 1	2.16
SB2	297–595	1569 ± 640	646 ± 166	2.43
SB3	250–297	921 ± 399	405 ± 143	2.27
SB4	< 250	392 ± 148	220 ± 61	1.78

heating zones (90, 100 and 110 °C) and screw speed of 40 rpm. TPS/SB composites (Figure 1d) were prepared under the same conditions as pure TPS with the addition of 10 wt% of SB fibers related to the mass of the corn starch.

2.4 Characterization

The size distribution of SB fibers was determined through optical microscopy images (Coleman, DN 107), using ImageJ 1.48v software to measure the diameter (D) and the length (L) of more than 100 fibers of each size range. The aspect ratio (L/D) was calculated as the ratio between the average values of L and D.

Diffraction patterns of SB fibers and pure TPS were measured on an X-ray diffractometer (D8 Focus, Bruker AXS) with a CuKα radiation (λ = 0.1541 nm) at 40 kV and 40 mA. Data were collected from 2θ = 5–40° at a scan rate of 2° min^{-1}, with no background subtraction. The crystallinity index (CI) of SB fibers was determined using the empirical method proposed by Segal *et al.* [23] according to Equation 1, where I_{200} is the total intensity of the (200) lattice diffraction of cellulose Iβ and I_{am} is the intensity diffraction of the amorphous scattering.

$$CI(\%) = \frac{I_{200} - I_{am}}{I_{200}} \times 100 \qquad (1)$$

Infrared spectra were recorded on a PerkinElmer Frontier spectrometer (100 FT-IR). SB spectra were collected using a KBr mixture at a ratio of 1:100 and made into KBr disks, prepared immediately before measurements. Spectra of pure TPS and TPS/SB composites were collected using the attenuated total reflection (ATR) mode. Bands were recorded in the region from 4000 to 650 cm^{-1}, with 4 cm^{-1} resolution and 32 scans.

The moisture content of SB fibers and TPS/SB composites was determined in triplicate, following the standard method of AOAC (1997) [24]. Samples of 0.3 g each were dried in a previously weighted test container at 100 °C for pure TPS and 110 °C for SB and TPS/SB composites for 30 min. After being cooled in a desiccator, samples were weighted and returned to the oven for another 30 min. This procedure was repeated until constant mass was reached. The moisture content was calculated according to Equation 2, where m_i is the initial mass of the sample, before drying, and m_d is the final mass after drying.

$$Moisture\ content(\%) = \frac{m_i - m_d}{m_i} \times 100 \quad (2)$$

To measure the moisture absorption of samples, dried samples (m_d) were conditioned in hermetic containers with a controlled environment (23 °C, 55% RH) using a saturated solution of calcium chloride. The amount of water absorbed by the samples was determined by periodical weighing, until constant mass was reached (m_f). The moisture absorbed by each sample was calculated according to Equation 3.

$$\text{Moisture absorption}(\%) = \frac{m_f - m_d}{m_d} \times 100 \quad (3)$$

To study the mechanical properties of pure TPS and TPS/SB composites, films of 10 mm × 80 mm × 0.3 mm were prepared from the extruded samples by compression molding (110 °C, 3 ton for 1 min). Tensile test (ASTM D882-95a) was performed in MTS Tytron 250 equipment, with distance between grips of 50 mm and rate of 5 mm/min.

The cryogenic fracture surface of the composites was characterized by scanning electron microscopy (SEM), using a JEOL-JSM-6010LA microscope instrument after gold coating using a Bal-Tec Multi Coating System MED020.

3 RESULTS AND DISCUSSION

The size distribution of SB fibers sifted in sieves with different granulometry is shown in Figure 2. It is possible to observe that SB fibers were efficiently separated into four size ranges. For the length, the distribution ranges become broader from SB1 to SB3 as fiber size decreases, while for the diameter the distribution ranges become narrower as the granulometry of sieves decreases.

The average values of L and D and the obtained aspect ratio (L/D) for each size range of SB fibers are related in Table 1. SB2 shows the highest aspect ratio, while SB4 shows the lowest value.

X-ray diffraction patterns of SB and TPS samples are shown in Figure 3. SB fibers (Figure 3a) show peaks at $2\theta = 15.8°$, $21.8°$ and $34.4°$. The peak at $2\theta = 15.8°$ is a convolution of two peaks at around $2\theta = 14.8°$ and $16.6°$, related respectively to the crystalline plans (110) and (1–10) of native cellulose Iβ [25]. The major peak at $21.8°$ 2θ is associated with the (200) crystalline plan of cellulose Iβ, while the small peak at $34.8°$ 2θ is attributed to the overlap of several neighboring reflections including (004) [25, 26]. The calculated crystallinity
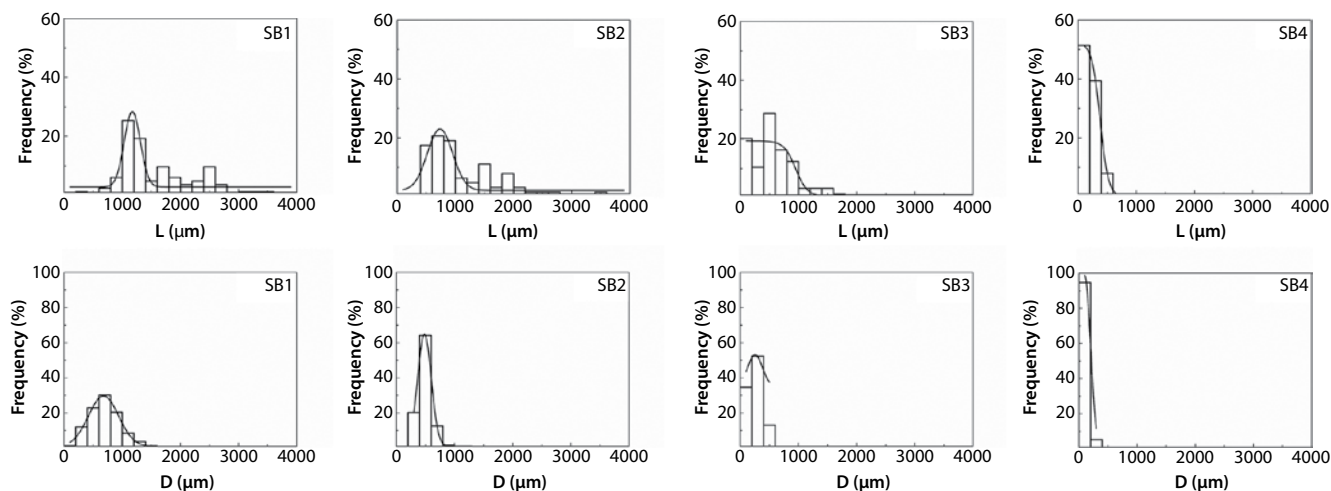

Figure 2 Distribution range of length (L) and diameter (D) for SB1, SB2, SB3 and SB4.
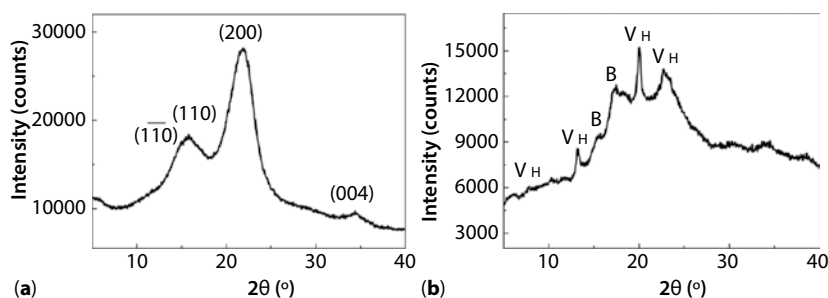

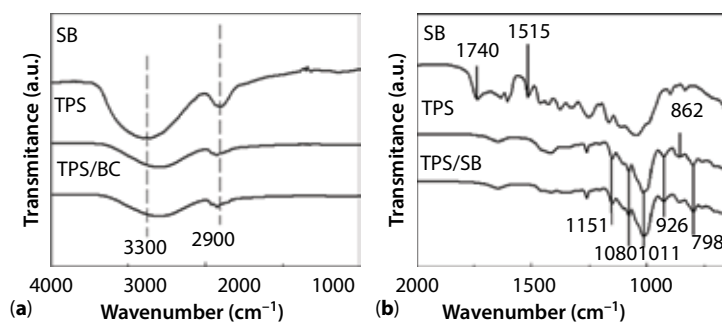**Figure 3** X-ray diffraction patterns of (**a**) SB and (**b**) TPS.

Figure 4 FTIR spectra of SB, TPS and TPS/SB composites in the (**a**) 2000-650 cm^{-1} and (**b**) 2000–650 cm^{-1} regions.

index of SB fibers was 44.9%, which is in accordance with the literature [27].

Corn TPS (Figure 3b) shows peaks at $2\theta = 7.8°$ (V_H), 13.2° (V_H), 15.8° (B), 17.5° (B), 20.0° (V_H) and 22.7° (V_H). While V_H crystal structure consists of amylose recrystallization induced by glycerol during the cooling of the processed material, the presence of peaks characteristic of B-type crystallization indicates residual crystallinity due to granules after the extrusion, attributed to the recrystallization of amylopectin [18, 28]. One of the major factors that influences the relative abundances of starch crystal structures is the amylose:amylopectin ratio [29], where the V_H crystallinity is proportional to amylose content for corn starch [30]. Also, the rate of change that is influenced by temperature and humidity during processing and the concentration of lysophospholipids and complex-forming agents as glycerol interfere in amylose crystallization. Overall, residual crystallinity within the residual granules leads to lower strength of TPS [29].

The FTIR spectra of SB, TPS and TPS/SB composites are shown in Figure 4. The full spectra in the region of 4000-650 cm^{-1} is shown in Figure 4a and the "fingerprint" region in which several stretching vibrations of different groups are present at 2000–650 cm^{-1} is shown in Figure 4b [31]. The SB spectrum shows characteristic peaks of cellulose, hemicellulose and lignin. The region from 3000–2800 cm^{-1} is ascribed to CH$_3$ and CH$_2$ asymmetrical and symmetrical stretching in cellulose [31–33], the peak at 1740 cm^{-1} is attributed to carbonyl groups (C=O) of uronic acids from hemicellulosic component [34]. The peaks at 1604 and 1515 cm^{-1} are related to C=C and C-O stretching or bending vibrations of different groups, such as breathing of the aromatic rings, which can be affected by the presence of substituents present in lignin [31]. Corn TPS spectrum shows bands at 1151, 1080 and 1011 cm^{-1} ascribed to C-O bond stretching and at 926, 862 and 798 cm^{-1} due to the entire anhydroglucose ring stretching vibrations [35]. TPS/SB spectrum has bands present both in SB and TPS spectra. All spectra show similar bands at the region from 3700 to 3000 cm^{-1} related to the strong

Table 2 Moisture content and absorption of SB, TPS and TPS/SB composites.

Sample	Moisture content (%)	Moisture absorption (%)
TPS	11.26 ± 0.04	11.85 ± 0.27
SBl	13.15 ± 0.08	7.29 ± 0.28
SB2	14.03 ± 0.01	6.89 ± 0.06
SB3	16.04 ± 0.01	6.76 ± 0.05
SB4	16.03 ± 0.02	5.76 ± 0.26
TPS/SB 1	18.75 ± 0.01	12.54 ± 1.55
TPS/SB2	14.74 ± 0.01	11.46 ± 0.13
TPS/SB3	18.38 ± 0.01	13.24 ± 0.55
TPS/SB4	16.07 ± 0.01	11.55 ± 1.21

hydrogen-bonded O-H stretching vibrations arising from inter- and intramolecular hydrogen bond [32], and around 1640 cm^{-1} assigned to the bending of O-H of water [36].

The moisture content and absorption of each size range of SB, TPS and TPS/SB composites are listed in Table 2. SB fibers have higher moisture content than TPS, and the lower the SB fibers' dimensions, the higher is their moisture content due to the higher surface area. As seen in FTIR results, TPS and SB show bands related to O-H bonding, which confers hydrophilic behavior for both matrix and disperse phase, which suggests favorable interaction between them.

The TPS/SB1 and TPS/SB3 composites show significantly higher moisture content than SB1 and SB3. It indicates that the intramolecular hydrogen bond between both SB and TPS with water molecules is more favorable than the interaction between the two phases. Conversely, TPS/SB2 and TPS/SB4 show almost the same moisture content as SB2 and SB4, which suggests the interaction between TPS and SB fibers is enhanced in the range of 297–595 µm and for SB fibers less than 250 µm. In this case, fewer OH groups from SB and TPS are available to interact with the OH groups of
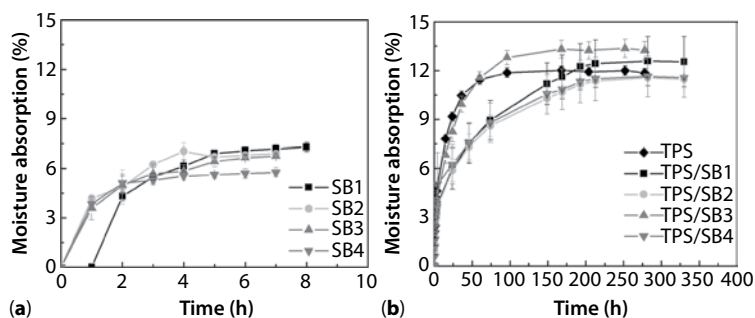
Figure 5 Moisture absorption of (**a**) SB fibers and (**b**) pure TPS and TPS/SB composites.

water, resulting in lower moisture absorption when compared to TPS/SB1 and TPS/SB3 [37].

The moisture absorption (Figure 5) of SB fibers is significantly lower than that of TPS and TPS/SB composites, which is ascribed to the fact that starch is more hygroscopic than SB fibers [9, 38]. The value observed for TPS is in agreement with previously reported results [16]. The higher the SB fibers' dimensions, the higher their moisture absorption is, showing an unexpected trend that is opposite to their moisture content.

The SEM micrographs of the fragile fracture surface of TPS/SB composites are shown in Figure 6, which reveal a good dispersion of SB fibers in corn TPS (see also Figure 1s presented in the Supplementary Data). Fiber breakage is clearly shown in Figure 6a, and the absence of fiber pullout (indicated by the arrows in Figure 6a–d) may be attributed to fiber-matrix affinity, leading to good adhesion [18, 38].

The results of the tensile test (tensile strength (σ), Young's modulus (E) and elongation at break (ε)) of pure TPS and TPS/SB composites are presented in Table 3. The correspondent plots are presented in the Supplementary Data, Figure 2s. The tensile strength of corn TPS (0.83 MPa) is lower than reported in the literature (2.6 to 4 MPa) [16, 18], which may be attributed to the presence of residual crystallinity, as shown by XRD results [29]. Adjustments in processing parameters and/or in the plasticizer concentration may enhance the strength of corn TPS. For all TPS/SB composites, the addition of SB fibers significantly improved the stiffness of the material when compared to pure TPS. With the exception of TPS/SB1, all the composites also showed improved tensile strength, with a slight decrease in the elongation at break.

Overall, TPS/SB2 composite presented the best mechanical behavior. The addition of SB2 fibers, which had the highest aspect ratio, increased by more than 660% the Young's modulus and by more than 100% the tensile strength with respect to pure TPS, while leading to one of the lowest decreases in the
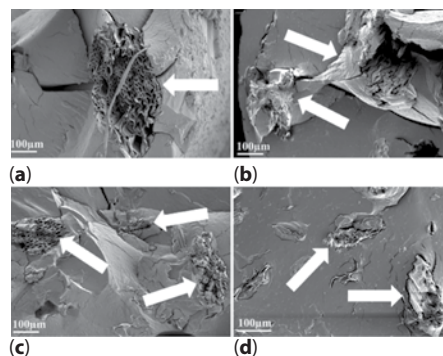

Figure 6 SEM micrographs of (**a**) TPS/SB1, (**b**) TPS/SB2, (**c**) TPS/SB3 and (**d**) TPS/SB4.

Table 3 Tensile properties of TPS and TPS/SB composites.

Sample	σ (MPa)	ε (%)	E (MPa)
TPS	0.83 ± 0.14	16.36 ± 3.83	6.71 ± 0.51
TPS/SBl	0.59 ± 0.04	10.06 ± 0.29	10.16 ± 0.91
TPS/SB2	1.73 ± 0.38	13.85 ± 1.99	44.36 ± 3.99
TPS/SB3	1.05 ± 0.09	10.24 ± 0.19	17.58 ± 1.40
TPS/SB4	1.70 ± 0.23	14.17 ± 1.40	22.55 ± 2.40

elongation at break. TPS/SB4 showed the second best mechanical behavior, where the addition of SB4 led to similar improvement of tensile strength but half of the stiffness improvement when compared to SB2. This result may be explained by the fact that although SB4 has lower dimensions, thus presenting higher surface area to interact with TPS, the higher aspect ratio of SB favors stress transfer to the matrix. Following the same tendency, as SB3 has higher surface area than SB1, TPS/SB3 shows better mechanical properties than TPS/SB1, but lower than TPS/SB4 and TPS/SB2.

In summary, results suggest that although SB fibers have good interaction with corn TPS, the mechanical behavior of TPS/SB composites results in a balance between aspect ratio and surface area of SB fibers. Even

Márcia Aparecida da Silva Spinacé et al.: Influence of Sugarcane Bagasse Fiber Size on Biodegradable

in the case of fiber size ranges with small differences between them, significant variation in the mechanical behavior of TPS/SB composites was verified. The improvements in TPS mechanical properties due to SB fibers addition shown in this study are higher than results reported earlier, where the tensile strength and Young's modulus increased only up to 146 and 340%, respectively [18, 19]. It can be attributed, first, to the use of fibers with a narrow size range distribution that allows the obtainment of a homogeneous composite, where fibers are capable of being uniformly distributed in the matrix [18]. Second, processing TPS composites via extrusion avoids the formation of fibrous agglomerates, being a time-saving process that allows large-scale production of TPS products with generation of few residues. Among the size ranges of SB fibers studied in this work, 297–595 µm (SB2) appeared to be the optimal size to improve the mechanical properties of biodegradable TPS/SB composites, optimizing the adhesion between fiber-matrix and leading to a better stress transfer between them.

4 CONCLUSIONS

The influence of four size ranges of SB fiber in the mechanical properties of biodegradable composites of TPS was studied. The addition of SB fibers led to significant improvements in both Young's modulus and tensile strength, with a slight decrease in the tensile strain. The enhancement of TPS mechanical properties with the addition of SB fibers is attributed to the good interaction between them, as suggested by SEM and tensile test results. The optimal SB size range appeared to be 297–595 µm (SB2), obtained when the fibers were sifted in sieves between 30 and 50 mesh. For TPS/SB2 composites, increases of more than 660% in the Young's modulus and more than 100% in the tensile strength were verified with respect to the pure TPS.

ACKNOWLEDGMENTS

REFERENCES

1. CONAB - Companhia Nacional de Abastecimento, Cana-de-açúcar: acompanhamento da safra brasileira, safra 2017/2018, segundo levantamento, http://www.conab.gov.br/OlalaCMS/uploads/arquivos/17_08_24_08_59_54_boletim_cana_portugues_-_2o_lev_-_17-18.pdf (2017).

2. D.A. Cerqueira, G. Rodrigues Filho, and C.S. Meireles, Optimization of sugarcane bagasse cellulose acetylation. *Carbohydr. Polym* **69**, 579–582 (2007).

3. K. Hofsetz and M.A. Silva, Brazilian sugarcane bagasse: Energy and non-energy consumption. *Biomass Bioenerg* **46**, 564–573 (2012).

4. B.S. Purchase, S. Rosettenstein, and D.V. Bezuidenhoudt, Challenges and potential solutions for storage of large quantities of bagasse for power generation. *Proc. S. Afr. Sug. Technol. Ass.* **86**, 495–513 (2013).

5. G. Eggleston and I. Lima, Sustainability issues and opportunities in the sugar and sugar-bioproduct industries. *Sustainability* **7**, 12209–12235 (2015).

6. N. Boonmee and P. Pongsamana, Spontaneous ignition of bagasse stockpiles in Thailand: A fire safety concern. *Eng. J.* **21**, 37–50 (2017).

7. D.A. Iryani, S. Kumagai, M. Nonaka, K. Sasaki, and T. Hirajima, Characterization and production of solid biofuel from sugarcane bagasse by hydrothermal carbonization. *Waste Biomass Valor* **8**, 1941–1951 (2017).

8. Y.R. Loh, D. Sujan, M.E. Rahman, and C.A. Das, Sugarcane bagasse – the future composite material: A literature review. *Resour. Conserv. Recy.* **75**, 14–22 (2013).

9. A. Pandey, C.R. Soccol, P. Nigam, and V.T. Soccol, Biotechnological potential of agro-industrial residues. I: Sugarcane bagasse. *Bioresour. Technol.* **74**, 69–80 (2000).

10. O. Faruk, A.K. Bledzki, H.-P. Fink, and M. Sain, Progress report on natural fiber reinforced composites. *Macromol. Mater. Eng.* **299**, 9–26 (2014).

11. S.N. Walford, Sugarcane bagasse: How easy is it to measure its constituents? *Proc. S. Afr. Sug. Technol. Ass.* **81**, 266–273 (2008).

12. F. Xie, P.J. Halley, and L. Avérous, Rheology to understand and optimize processibility, structures and properties of starch polymeric materials. *Prog. Polym. Sci.* **37**, 595–623 (2012).

13. A.P. Teodoro, S. Mali, N. Romero, and G.M. Carvalho, Cassava starch films containing acetylated starch nanoparticles as reinforcement: physical and mechanical characterization. *Carbohydr. Polym.* **126**, 9–16 (2015).

14. S. Shibata, Y. Cao, and I. Fukumoto, Press forming of short natural fiber-reinforced biodegradable resin: Effects of fiber volume and length on flexural properties. *Polym. Test* **24**, 1005–1011 (2005).

15. Y. Cao, S. Shibata, and I. Fukumoto, Mechanical properties of biodegradable composites reinforced with bagasse fiber before and after alkali treatments. *Compos. Part A-Appl. S* **37**, 423–429 (2006).

16. J.L. Guimarães, F. Wypych, C.K. Saul, L.P. Ramos, and K.G. Satyanarayana, Studies of the processing and characterization of corn starch and its composites with banana and sugarcane fibers from Brazil. *Carbohydr. Polym* **80**, 130–138 (2010).

17. F. Debiagi, S. Mali, M.V.E. Grossmann, and F. Yamashita, Effects of vegetal fibers on properties of cassava starch biodegradable composites produced by extrusion. *Ciênc. Agrotec* **34**, 1522–1529 (2010).

18. M.E. Vallejos, A.A.S. Curvelo, E.M. Teixeira, F.M. Mendes, A.J.F. Carvalho, F.E. Felissia, and M.C. Area, Composite materials of thermoplastic starch and fibers

from the ethanol–water fractionation of bagasse. *Ind. Crop. Prod.* **33**, 739–746 (2011).

19. T. Galicia-García, F. Martínez-Bustos, O.A. Jiménez-Arévalo, D. Arencón, J. Gámez-Pérez, and A.B. Martínez, Films of native and modified starch reinforced with fiber: influence of some extrusion variables using response surface methodology. *J. Appl. Polym. Sci.* **126**, E327–E336 (2012).

20. W.N. Gilfillan, D.M.T. Nguyen, P.A. Sopade, and W.O.S. Doherty, Preparation and characterisation of composites from starch and sugarcane fiber. *Ind. Crop. Prod.* **40**, 45–54 (2012).

21. W.N. Gilfillan, P.A. Sopade, and W.O.S. Doherty, Moisture uptake and tensile properties of starch-sugarcane fiber films. *Int. Sugar J.* **115**, 23–27 (2013).

22. D. N. Saheb and J. P. Jog, Natural fiber polymer composites: A review. *Adv. Polym. Tech.* **18**, 351–363 (1999).

23. L. Segal, J.J. Creely, A.E. Martin, and C.M. Conrad, An empirical method for estimating the degree of crystallinity of native cellulose using X-ray diffractometer. *Tex. Res. J.* **29**, 786–794 (1959).

24. Official methods of analysis of AOAC International, AOAC (1997).

25. A.D. French, Idealized powder diffraction patterns for cellulose polymorphs. *Cellulose* **21**, 885–896 (2014).

26. S. Nam, A.D. French, B.D. Condon, and M. Concha, Segal crystallinity index revisited by the simulation of X-ray diffraction patterns of cotton cellulose Iβ and cellulose II. *Carbohydr. Polym.* **135**, 1–9 (2016).

27. A.A. Guilherme, P.V.F. Dantas, E.S. Santos, F.A.N. Fernandes, and G.R. Macedo, Evaluation of composition, characterization and enzymatic hydrolysis of pretreated sugar cane bagasse. *Braz. J. Chem. Eng.* **32**, 23–33 (2015).

28. E.M. Teixeira, C. Lotti, A.C Corrêa, K.B. Teodoro, J.M. Marconcini, and L.H. Mattoso, Thermoplastic corn starch reinforced with cotton cellulose nanofibers. *J. Appl. Polym. Sci.* **120**, 2428–2433 (2011).

29. J.J.G. Van Soest and J.F.G. Vliegenthart, Crystallinity in starch plastics: Consequences for material properties. *Trends Biotechnol.* **15**, 208–213 (1997).

30. E.M. Teixeira, D. Róz, A. Luzia, A.J.F de Carvalho, and A.A.S. Curvelo, Preparation and characterisation of thermoplastic starches from cassava starch, cassava root and cassava bagasse. *Macromol. Symp.* **229**, 266–275 (2005).

31. M. Poletto, A. Zattera, and R.M.C. Santana, Structural differences between wood species: Evidence from chemical composition, FTIR spectroscopy and thermogravimetric analysis. *J. Appl. Polym. Sci.* **126**, E336–E344 (2012).

32. Y. Li, G. Li, Y. Zou, Q. Zhou, and X. Lian, Preparation and characterization of cellulose nanofibers from partly mercerized cotton by mixed acid hydrolysis. *Cellulose* **21**, 301–309 (2014).

33. C.M. Popescu, G. Singurel, M.C. Popescu, C. Vasile, D.S. Argyropoulos, and S. Willför, Vibrational spectroscopy and X-ray diffraction methods to establish the differences between hardwood and softwood. *Carbohydr. Polym.* **77**, 851–857 (2009).

34. A.M. Adel, Z.H. Abd El-Wahab, A.A. Ibrahim, and M.T. Al-Shemy, Characterization of microcrystalline cellulose prepared from lignocellulosic materials. Part I. Acid catalyzed hydrolysis. *Bioresource Technol.* **101**, 4446–4455 (2010).

35. H. Chi, K. Xu, X. Wu, Q. Chen, D. Xue, C. Song, W. Zhang, and P. Wang, Effect of acetylation on the properties of corn starch. *Food Chem.* **106**, 923–928 (2008).

36. Y.X. Xu, K.M. Kim, M.A. Hanna, and D. Nag, Chitosan–starch composite film: Preparation and characterization. *Ind. Crop. Prod.* **21**, 185–192 (2005).

37. A.L.D Róz, P. Veiga-Santos, A.M. Ferreira, T.C.R. Antunes, F.D.L. Leite, F.M. Yamaji, and A.J.F.D. Carvalho, Water susceptibility and mechanical properties of thermoplastic starch–pectin blends reactively extruded with edible citric acid. *Mat. Res.* **19**, 138–142 (2016).

38. A.A.S. Curvelo, A.J.F. De Carvalho, and J.A.M. Agnelli, Thermoplastic starch–cellulosic fibers composites: preliminary results. *Carbohydr. Polym.* **45**, 183–188 (2001).

Supplementary Document Available Online

http://www.scrivenerpublishing.com/images/JRM/JRM-2017-0110/jrm_JRM-2017-0110_supp1.pdf

sp